Gaining insight into the T_2*-T_2 relationship through complex inversion of surface NMR free-induction decay data

Denys Grombacher* *Aarhus University* *C.F. Mollers Alle 4, Aarhus, DK* *denys.grombacher@geo.au.dk*

Esben Auken *Aarhus University* *C.F. Mollers Alle 4, Aarhus, DK* *esben.auken@geo.au.dk*

SUMMARY

One of the primary shortcomings of the standard surface nuclear magnetic resonance (NMR) measurement, called the free-induction decay (FID), is the uncertainty about the link between the signal's time dependence and the geometry of the pore space. Ideally, the FID signal's time dependence, described by the parameter T_2*, carries an intimate link to the geometry of the pore space allowing robust estimation of pore-size and permeability. However, T_2* can also be strongly influenced by background magnetic field (B_0) inhomogeneity, which can mask the link to pore geometry. To improve the utility of surface NMR FID measurements, we investigate whether complex inversion of surface NMR data can be used to provide insight into the link between T_2* and T_2 (the parameter carrying the link to pore geometry). Synthetic and field measurements are presented to demonstrate that an alternative forward modelling approach that involves direct modelling of relaxation during pulse (RDP) effects can help constrain the relationship between T_2* and T_2. Complex inversions are performed using forward models that include RDP for varying magnitudes of B_0 inhomogeneity (consistent with observed T_2* values) and it is observed that satisfactory data fits can only be obtained given reliable T_2 estimates. Thus providing insight into the T_2*-T_2 relationship. We aim to demonstrate that an alternative forward modelling approach may help improve the utility of FID measurements for estimation of pore-scale properties.

Key words: hydrogeophysics, nuclear magnetic resonance

INTRODUCTION

One of the primary shortcomings of the standard surface NMR measurement, the free-induction decay (FID), is the uncertainty surrounding which mechanism controls the signal's time-dependence. Under ideal conditions the FID's time-dependence, described by a relaxation time called T_2*, carries a strong link to the geometry of the pore space. This link to pore space geometry is the basis for NMR-based permeability estimates, which have been widely exploited in the petroleum industry for decades. The challenge in surface NMR is that in the presence of a heterogeneous background magnetic field (B_0) a mechanism called dephasing also contributes to the observed decay potentially masking the connection to pore geometry (Grunewald and Knight, 2011). If the role of dephasing is neglected it may lead to biased/inaccurate estimates of permeability. The difficulty is that given only FID measurements it is extremely difficult to determine which mechanism controls T_2*, and therefore, if T_2* can be reliably used to estimate permeability. To improve surface NMR's links to pore geometry much work has focused on developing surface NMR experimental protocols capable of directly measuring alternative relaxation times, called T_2 and T_1, that are less/not influenced by dephasing (Legchenko et al., 2010; Walbrecker et al., 2011; Grunewald and Walsh, 2013;). Despite the successes of these techniques the FID remains the standard measurement due to its reduced collection times and increased penetration depths.

The difference between T_2* and T_2 is the impact of dephasing. If the influence of dephasing on T_2* could be quantified (i.e if the relationship between T_2 and T_2* could be constrained) it would represent a significant improvement in the utility of the FID for permeability estimation. We hypothesize that an updated scheme to handle relaxation during pulse effects, which describe the influence of T_2* on the excitation pulse, can be used to constrain the T_2*-T_2 relationship. Instead of solving the simplified Bloch equation without relaxation terms, as is standard in surface NMR, an updated forward model that solves the full Bloch equation is employed. This provides the forward model the flexibility to adjust based on the current estimate of T_2. In practice, the range of plausible T_2 can only be constrained to values larger than or equal to T_2*. We investigate whether forward responses based on different but plausible estimates of T_2 provide varying abilities to fit complex surface NMR data. We demonstrate that forward models based on poor/inaccurate estimates of T_2 produce reduced quality data fits, while forward models based on accurate T_2 estimates provide robust data fits. As such, examining the data fits for a range of plausible T_2 values can be used to provide an estimate of T_2; since the best data fits will correspond to best T_2 estimate. Synthetic and field data are presented to investigate the feasibility of such an approach, ultimately demonstrating that the updated forward model provides the ability to constrain the T_2*-T_2 relationship from FID data only.

METHODS AND RESULTS

The processes controlling the time-dependence of the FID signal also take place during the excitation pulse; the impact of these processes are referred to as relaxation during pulse (RDP) effects. Traditionally, RDP is not accounted for by modifying the forward model but instead accounted for by adjusting the time at which the initial amplitude of the signal is calculated (Walbrecker et al., 2009). In this work we employ an alternative scheme that instead attempts to account for RDP by solving the Bloch equations with appropriately weighted relaxation terms present (Grombacher et al., 2017). One complication of this updated scheme is that it

requires the relaxation times T_2 and T_1 to be estimated. The difficulty is that these parameters are poorly constrained given only FID data; the only limits on T_2/T_1 is that they must be larger than T_2* and less than approximately 1-1.5 s (the relaxation times for bulk water). However, we hypothesize that the flexibility to modify the forward model to reflect different T_2*-T_2 relationships may offer the potential to gain insight the true value of T_2. This hypothesis stems from a desire to exploit that RDP effects manifest differently depending on the true T_2*-T_2 scenario (Grombacher et al., 2017). Figure 1 highlights the sensitivity of the signal amplitude and phase to the T_2*-T_2 scenario. Each colored dot in Figure 1A corresponds to a plausible T_2-T_{2IH} pair (signal loss due to dephasing is described by the parameter T_{2IH}) consistent with a T_2* value of 80 ms. That is, given data with T_2* of 80 ms each dot represents an equally likely scenario; only the location of the T_2* contour (black line) in Figure 1A can be constrained by the data. To illustrate the possible variation in signal amplitude and phase for the different scenarios (colors), Figure 1B and 1C illustrate the real and imaginary sounding curves produced by a survey employing a 75 m coincident circular loop and a 40 ms 4 Hz off-resonance pulse. The subsurface is resistive and is a 20% water content half-space. All forward modelling/inversion in this study was performed using MRSmatlab (Müller-Petke et al., 2016). The curves demonstrate that significant variations in real and imaginary signal amplitudes are observed depending on whether the scenario is described by a strongly heterogeneous B_0 (red, large T_2) or a homogeneous B_0 (blue, small T_2). The difference profiles (1D and 1E) indicate that the amplitude variation can be as large as ~10-20% in this example.

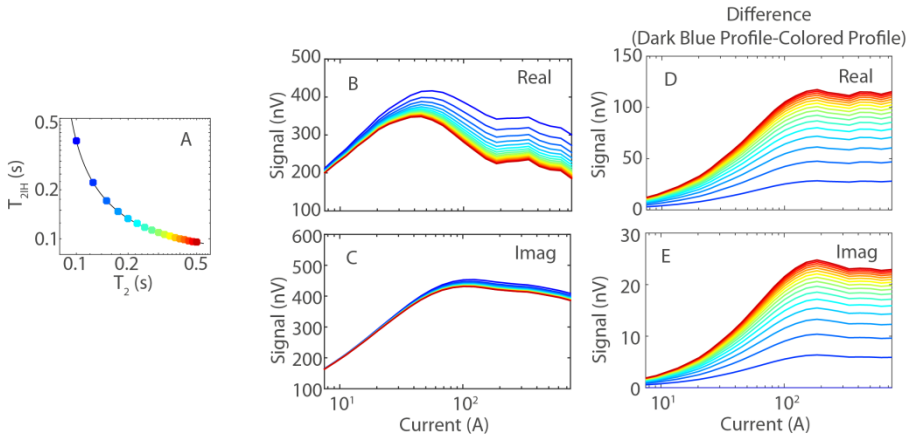

Figure 1. A) The range of plausible T_2-T_{2IH} combinations consistent with an observed T_2* of 80 ms. B) and C) illustrate the real and imaginary sounding curves. D) and E) illustrate the difference between each sounding curve and the most homogenous B_0 sounding curve (dark blue line). Colors correspond to a particular T_2-T_{2IH} combination indicated by the dot location/color in A).

Given the magnitude of variation observed in Figure 1, we hypothesize that inversions using forward models with an inaccurate T_2 estimate will struggle to accurately fit the signal amplitudes and phase. We propose a work flow where FID data is inverted multiple times, each time using a different kernel describing a plausible T_2-T_{2IH} pair. After the suite of inversions is completed, the resulting data fits produced by each case are compared. Kernels producing satisfactory data fits will be considered plausible T_2-T_{2IH} scenarios, while kernels that produce poor data fits will be used to identify unlikely T_2-T_{2IH} scenarios. Ideally, a narrow range of T_2 will provide satisfactory data fits, allowing the relationship between T_2* and T_2 to be constrained.

Consider a simple two layer model representative of an unconfined aquifer underlain by a low water content layer. A similar synthetic survey is performed using a 75 m coincident loop, the same excitation pulse as in Figure 1, and a resistive subsurface. The true water content profile is illustrated by the black line. Data is forward modelled with T_2*=80 ms and T_2=T_1=150 ms. All depth layers are given the same relaxation times. Ten nV of white Gaussian noise is added to the synthetic data. The resulting synthetic data is inverted using a suite of forward models, each corresponding to a different T_2-T_{2IH} pair. T_2 ranging from 100 ms to 500 ms in steps of 25 ms are investigated (same colors as in Figure 1). In each case, the magnitude of T_{2IH} (i.e. extent of B_0 heterogeneity) is selected to ensure T_2*=80 ms. The forward model assumes that each depth layer has the same T_2* and T_2. The suite of inversions is performed once using the standard amplitude-only inversion, and again using a complex-inversion that also attempts to fit the signal phase. The resulting water content profiles in each case are shown in the top row of Figure 2 (amplitude and complex-inversions in the left and right columns, respectively). The corresponding data fits for each T_2 estimate (real and imaginary χ^2 correspond to circles and stars, respectively) are illustrated in the bottom row. The true T_2 is indicated by the vertical dashed line.

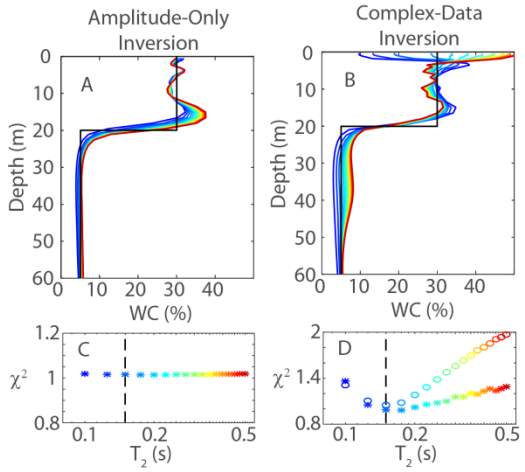

Figure 2. Water content profiles produced by a suite of inversions each with a forward model corresponding to a different plausible T_2-T_{2IH} pair (same colors as in Figure 1). The left and right columns correspond to amplitude-only and complex inversions, respectively. The true water content profile is shown by the black line.

Consider first the amplitude-only inversion. Each water content profile accurately reproduces the true water content profile and produces a satisfactory data fit. A small bias towards increased water content at the bottom of the upper layer is observed for the poorest T_2 estimates (red) but this bias is not reflected in the data fit. Instead, each inversion produces effectively the same level of data fit thus providing no insight into the true value of T_2 since the plausible range cannot be narrowed. Alternatively, the water content profiles for the complex inversion show more variation, particularly at the shallowest depths. The water content in the bottom layer also increases for poorer T_2 estimates (red). However, the data fits for the complex-inversions show a much stronger dependence on T_2 where a distinct minimum centered around the true T_2 can be observed. For poor T_2 estimates (dark blue and red) the complex-inversion struggles to accurately describe the signal phase resulting in poor data fits for both the real and imaginary components. The data fits allow the range of plausible T_2 to be far more tightly constrained. From the data fit alone, it is possible to determine that using T_2* directly for permeability estimation would produce biased estimates (since the T_2=100 ms case which is ~= T_2* of 80 ms produces a poor data fit). Additionally, the long T_2 estimates also struggle to fit the data. Beyond an increased χ^2 the poorer data fits are also easily identified by noting that consistent structure exists in data misfit plots. In summary, Figure 2 indicates that when combined with the complex inversion, the updated forward model that solves the full Bloch equations has the potential to help constrain the T_2*-T_2 relationship.

To investigate whether the proposed method is feasible under field conditions we present results for a two data sets collected at Leque Island, Washington. The data was collected by Dr. Elliot Grunewald using the Vista-Clara GMR system. A 40-m two turn circular coincident loop was employed. Two data sets were collected, the first using a 40 ms on-resonance excitation pulse with the second using an adiabatic excitation pulse described by the numerically optimized modulation approach discussed in Grombacher and Auken (2016). Thirty-six pulse moments ranging from ~0.1 As to ~8.5 As were employed in each case. In each case the data displayed T_2*~30 ms for all pulse moments. Using this observed T_2*, forward models were constructed for T_2 estimates of [50 100 150 200 250 300 400 500] ms; T_1=T_2 in all forward modelling. The forward model treats every depth layer with the same T_2* and T_2; this rough approximation is based on the consistent T_2* observed across nearly all pulse moments. Future implementation of the proposed method will allow the forward model to treat different depth layers with different T_2* and T_2 estimates. The current implementation represents a feasibility test that assumes a simple subsurface model. The resulting water content profiles are illustrated in Figure 3A and 3B, which correspond to the on-resonance and adiabatic pulse, respectively. The profile colors correspond to the T_2 value assumed by the forward model. Each water content profile is determined using a complex-inversion. Figures 3C and 3D illustrate the data fits corresponding to each water content profile. The estimated T_2* profiles are not shown, but demonstrate little structure and consistently show T_2*~=30 ms. Consider first the on-resonance case, where a distinct minima is observed to occur around 150-200 ms (green). The data fit degrades for smaller and higher T_2 estimates. For the adiabatic case, the data fit also shows a minimum around 200 ms (green), but with larger T_2 estimates still providing quality data fit as well; i.e. the χ^2 curve flattens at higher T_2. At the smallest T_2 (red/yellow) the data fit is again reduced. Similar behaviour is exhibited in both cases, poor data fits are produced at the smallest T_2 estimates, with good data fits occurring for T_2~200 ms. At longer T_2 only the on-resonance case shows degraded data fits. This may be a consequence that the particular adiabatic pulse employed is not particularly sensitive to T_2 changes in the long T_2 limit. Overall, the data fits in these two cases suggest that T_2 is likely ~200 ms. This estimate is close to results produced by an NMR T_2 log at the site, which also illustrated T_2 of ~150-300 ms at most depths. The similarity to nearby borehole T_2 estimates and the consistency between the two data sets collected using different excitation pulses serves to demonstrate the feasibility of the proposed approach under real field conditions.

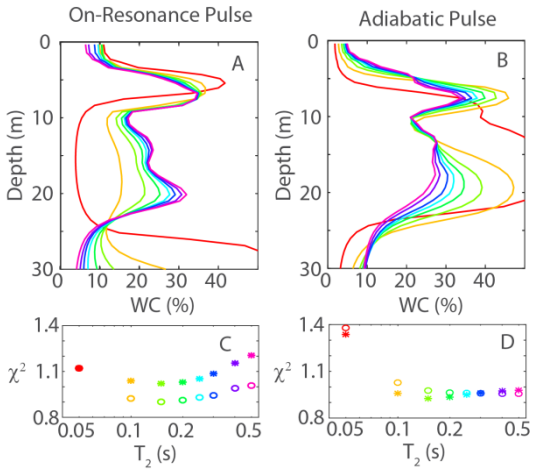

Figure 3. Water content profiles estimated at a site in Washington, USA. The left and right columns correspond to results produced by a 40 ms on-resonance pulse and an example adiabatic pulse, respectively. Profile colors correspond to results produced by an inversion that assumes a particular T_2 (the T_2 for each color is shown in the C) and D)). C) and D) illustrate the χ^2 for each inversion.

DISCUSSION

Taken together, the synthetic and field results in Figures 2 and 3 serve to demonstrate the potential to constrain the T_2*-T_2 relationship given only FID data. Similar abilities to estimate T_2 based on data fit are also observed for alternative synthetic case studies using different T_2*, T_2, and subsurface models. The depth of observed minima's are reduced for higher noise levels. The ability to resolve T_2 depends on the particular excitation pulse's sensitivity to RDP. Future work will investigate whether particular pulse types are well suited to resolving T_2 given this type of an inversion framework. Future work will also focus on improving the forward modelling/inversion scheme to allow for T_2* and T_2 to vary for different depth layers. This will likely require a non-linear

inversion where the forward modelling is based upon the current estimate of the T_2* depth profile, where an updated kernel will need to be formed after each iteration in the inversion.

CONCLUSIONS

An approach to constrain the relationship between T_2* and T_2 that uses an updated forward model that solves the full Bloch equation is presented. The approach requires estimation of T_2 and T_1, which are both poorly constrained in practice. To address this uncertainty, data is inverted using multiple forward models each containing a different but plausible T_2 estimate. Comparison of the data fits for the resulting suite of inversions is shown to demonstrate sensitivity to the true underlying T_2. That is, forward models given a poor estimate of the true T_2 produce poorer data fits for a complex-inversion than forward models given an accurate T_2 estimate. The amplitude-only inversion is shown to demonstrate significantly less sensitivity than the complex-inversion to the estimated T_2 in the forward model. Examination of the range of T_2 estimates that produce satisfactory data fits allows the plausible range of T_2 to be further constrained and provides valuable insight into the T_2*-T_2 relationship. The feasibility of the approach, using a simplified implementation that treats the entire subsurface with a single T_2* and T_2 estimate, is shown to accurately describe complex-valued field data collected at a site in Washington, USA, while also estimating a T_2 consistent with nearby logging NMR measurements. Overall, the proposed approach has great potential to improve the value of the standard FID measurement.

ACKNOWLEDGMENTS

D. Grombacher was supported by funding from the Danish Council for Independent Research (DFF-5051-00002). MRSmatlab was used for all forward modelling/inversion of surface NMR data (Müller-Petke et al., 2016).

REFERENCES

Grombacher, D., and Auken, E., 2016, Designing adiabatic pulses for surface NMR: ASEG extended abstracts 2016 (https://doi.org/10.1071/ASEG2016ab199).

Grombacher, D., Behroozmand, A.A., and Auken, E., 2017, Accounting for relaxation during pulse effects for long pulses and fast relaxation times in surface NMR: Geophysics, (https://doi.org/10.1190/geo2016-0567.1).

Grunewald, E., and Knight, R., 2011, The effect of pore size and magnetic susceptibility on the surface NMR relaxation parameter T_2*: Near Surface Geophysics, 9 (2), 169-178.

Grunewald, E., and Walsh, D., 2013, Multiecho scheme advances surface NMR for aquifer characterization: Geophysical Research Letters, 40 (24), 6346-6350.

Legchenko, A., Vouillamoz, J-M., and Roy, J., 2010, Application of the magnetic resonance sounding method to the investigation of aquifers in the presence of magnetic materials: Geophysics, 75 (6), L91-L100.

Müller-Petke, M., Braun, M., Hertrich, M., Costabel, S., and Walbrecker, J., 2016, MRSmatlab – A software tool for processing, modeling, and inversion of magnetic resonance sounding data: Geophysics, 81 (4), WB9-WB21.

Walbrecker, J., Hertrich, M., and Green, A.G., 2009, Accounting for relaxation processes during the pulse in surface NMR data: Geophysics, 74 (6), G27-G34.

Walbrecker, J., Hertrich, M., Lehmann-Horn, J.A., and Green, A.G., 2011, Estimating the longitudinal relaxation time T_1 in surface NMR: Geophysics, 76 (2), F111-F122.